The Journal of Chemical Physics

RAPID COMMUNICATION | NOVEMBER 12 2018

Communication: Substantial impact of the orientation of transition dipole moments on the dynamics of diatomics in laser fields FREE

Péter Badankó; Gábor J. Halász; Lorenz S. Cederbaum ; Ágnes Vibók ; András Csehi

J. Chem. Phys. 149, 181101 (2018)
https://doi.org/10.1063/1.5054775

Communication: Substantial impact of the orientation of transition dipole moments on the dynamics of diatomics in laser fields

Péter Badankó,[1] Gábor J. Halász,[2] Lorenz S. Cederbaum,[3] Ágnes Vibók,[1,4,a)] and András Csehi[1,4,b)]

[1]*Department of Theoretical Physics, University of Debrecen, P.O. Box 400, H-4002 Debrecen, Hungary*
[2]*Department of Information Technology, University of Debrecen, P.O. Box 400, H-4002 Debrecen, Hungary*
[3]*Theoretical Chemistry, Institute of Physical Chemistry, University of Heidelberg, D-69120 Heidelberg, Germany*
[4]*ELI-ALPS, ELI-HU Non-Profit Ltd., Dugonics tér 13, H-6720 Szeged, Hungary*

(Received 3 September 2018; accepted 30 October 2018; published online 12 November 2018; publisher error corrected 13 November 2018)

The formation of light-induced conical intersections (LICIs) between electronic states of diatomic molecules has been thoroughly investigated over the past decade. In the case of running laser waves, the rotational, vibrational, and electronic motions couple via the LICI giving rise to strong nonadiabatic phenomena. In contrast to natural conical intersections (CIs) which are given by nature and hard to manipulate, the characteristics of LICIs are easily modified by the parameters of the laser field. The internuclear position of the created LICI is determined by the laser energy, while the angular position is given by the orientation of the transition dipole moment (TDM) with respect to the molecular axis. In the present communication, using MgH^+ as a showcase example, we exploit the strong impact of the orientation of the TDMs exerted on the light-induced nonadiabatic dynamics. Comparing the photodissociations induced by parallel or perpendicular transitions, a clear signature of the created LICIs is revealed in the angular distribution of the photofragments. *Published by AIP Publishing.* https://doi.org/10.1063/1.5054775

Conical intersections (CIs)—the primary cause for nonadiabatic dynamics in polyatomic molecules—play a very important role in different fields of physics and chemistry. However, according to the well-known non-crossing rule, conical intersections are not available in diatomic molecules in field-free space.

At a CI, the nonadiabatic couplings become singular, giving rise to intense nonadiabatic effects widely studied in the literature.[1–7] In several fundamental chemical dynamical phenomena such as vision, photosynthesis, or the photochemistry of DNA, CIs serve as efficient and ultrafast channels for the decay processes. These naturally occurring CIs are not isolated points in the nuclear configuration space but rather form a seam of 3N-8 dimensions (N is the number of atoms). Clearly, the position of natural CIs and the strength of the related nonadiabatic couplings are inherent properties of the electronic states of a molecule and are difficult to manipulate.[8,9]

However, when molecules are exposed to resonant laser light, a new feature emerges. This feature is a CI induced by the light which cannot be avoided even in the case of diatomic molecules.[10,11] The angle θ between the laser polarization and the molecular axis provides the missing dynamical variable that together with the vibrational coordinate constitutes the branching space in which the induced CI can exist. We note here that this phenomenon is general and not restricted to running waves. Light-induced conical intersections (LICIs) can also emerge in standing waves which form optical lattices[10] widely used in cold-atom physics.

The internuclear position of LICIs is determined by the laser frequency, while the angular position is defined by the orientation of the transition dipole moment (TDM). Furthermore, the laser intensity controls the strength of the nonadiabatic couplings associated with the LICI. Consequently, the characteristics of LICIs are easily manipulated by the laser parameters.[11]

In the past decade, numerous theoretical[12–23] and experimental[24] studies have demonstrated the strong impact of LICIs on the spectroscopic and dynamical properties of diatomic molecules. In particular, two robust effects served as direct signatures for LICIs—one found in the angular distribution of the D_2^+ fragments[18] and one in the field-dressed spectra of the Na_2 molecule.[23] Owing to the large number of vibrational coordinates, LICIs are ubiquitous in polyatomic molecules. They become multidimensional in the nuclear coordinate space, opening the door for manipulating and controlling nonadiabatic effects with light.[25]

Recently, the competition between intrinsic and light-induced nonadiabatic phenomena in strongly coupled diatomics such as NaI and LiF has been reported.[26–28] In these studies, the LICI was found to provide a very efficient pathway for extremely fast population transfer between the electronic states under consideration.

In this communication, we go beyond previous investigations and study a physical event that can provide a new direct observable signature of light-induced conical intersections. Studying the MgH^+ molecular ion[29–37] as a showcase

a)vibok@phys.unideb.hu
b)csehi.andras@science.unideb.hu

example, our principal aim is to reveal the laser-induced nonadiabatic dynamics from the TDM orientation point of view. More precisely, we simulate the photodissociation of this system induced by perpendicular ($\Sigma \rightarrow \Pi$) and parallel ($\Sigma \rightarrow \Sigma$) transitions. Depending on the orientation of the TDMs, the angular position of the induced CI occurs at different laser-molecule orientations, which is expected to have a fingerprint in the angular distribution of the photofragments. The present paper is therefore devoted to the detailed investigation of this phenomenon.

In our nuclear dynamical study, two low-lying electronic states of MgH^+, the $^1\Sigma^+$ ground and the $^1\Pi$ second excited states are considered (labeled as Σ_1 and Π_1, respectively; see Fig. 1). The full time-dependent nuclear Hamiltonian of MgH^+ in the space of these two electronic states is a 3×3 matrix. However, as the Π_1 state is degenerate, one can, depending on the field polarization, transform it to a state which couples to the Σ_1 and a state which decouples from the dynamics. The resulting 2×2 Hamiltonian then reads

$$\hat{H}(t) = \left(-\frac{1}{2M_r}\frac{\partial^2}{\partial R^2} + \frac{1}{2M_r R^2}L_\theta^2\right)\mathbf{1} + \begin{pmatrix} V_{\Sigma_1} & 0 \\ 0 & V_{\Pi_1} \end{pmatrix} - E_0\cos(\omega t)\cdot\sin^2(\pi t/T)\begin{pmatrix} \mu_{\Sigma_1}\cos\theta & \mu_{\Sigma_1\Pi_1}\sin\theta \\ \mu_{\Sigma_1\Pi_1}\sin\theta & \mu_{\Pi_1}\cos\theta \end{pmatrix}. \quad (1)$$

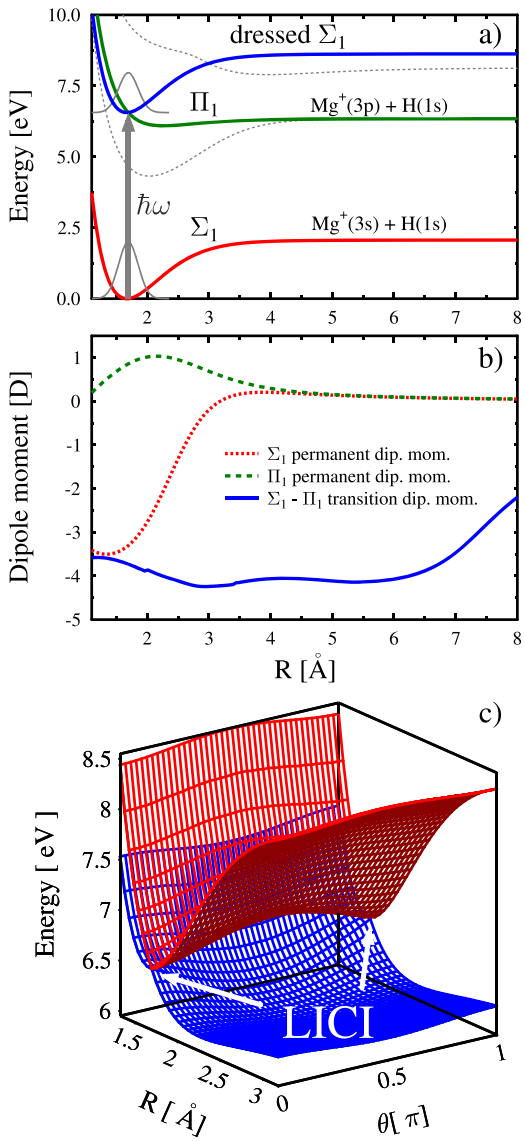

FIG. 1. (a) Field-free potential energy curves of the Σ_1 (red line) and Π_1 (green line) electronic states of the MgH^+ molecular ion applied in the present dynamical treatment. The light-dressed ground state is presented by the solid blue line. The dashed gray lines show further singlet Σ states. (b) Permanent dipole moments of the considered Σ_1 (red dashed line) and Π_1 (green dashed line) states, as well as the corresponding $\Sigma_1 \rightarrow \Pi_1$ transition dipole moment function (solid blue line). (c) Dressed adiabatic lower (blue) and upper (red) potential energy surfaces for the perpendicular $\Sigma_1 \rightarrow \Pi_1$ transition in MgH^+ representing the LICIs at $\theta = 0$ and $\theta = \pi$.

On the right-hand side of Eq. (1), the first term includes the vibrational and rotational kinetic energy operators with M_r being the reduced mass and R being the internuclear distance. L_θ is the angular momentum operator (the Hamiltonian conserves the projection m of the angular momentum) and θ is the angle between the molecular axis and the laser polarization. In the second term, V_{Σ_1} and V_{Π_1} are the potential energies corresponding to the Σ_1 and Π_1 electronic states, respectively. The third term describes the interaction with the laser field in the dipole approximation. Here, E_0 is the electric field amplitude, ω is the frequency, while T is the pulse duration. μ_{Σ_1} and μ_{Π_1} denote the permanent dipoles, while $\mu_{\Sigma_1\Pi_1}$ is the transition dipole moment between the two electronic states. Equation (1) describes rotating-vibrating molecules (2D simulations), but we will make comparisons to the so-called 1D simulations where the rotation is frozen. The correct 1D calculation to describe a molecule in a laser field requires averaging over numerous computations done for different values of the θ parameter. This approach is also necessary for comparison with the full (i.e., 2D) solution of the problem where both R and θ are treated as dynamical variables.

For MgH^+, the TDM between the Σ_1 and Π_1 states is perpendicular to the molecular axis and, hence, also to the permanent dipoles. From now on, we refer to this system as the "real system." In order to study the impact of the direction of the TDM, we define a "model system" in which the $\Sigma \rightarrow \Pi$ TDM is artificially twisted parallel to the molecular axis as if it were a $\Sigma \rightarrow \Sigma$ TDM. The corresponding Hamiltonian is the same as in Eq. (1), except for the last term, in which the $\sin\theta$ factors are changed to $\cos\theta$ accordingly.

All the numerical results presented in this work have been determined by employing the full Hamiltonian in Eq. (1). However, before proceeding further, we would like to elucidate the emergence of LICIs for both perpendicular and parallel transitions. For that purpose, it is useful to simplify and reduce the Hamiltonian further. First, the so-called dressed state representation[38] is used. Since the laser frequency employed is high, one may neglect the permanent dipoles in Eq. (1) which average to zero in high-frequency fields[25] and, furthermore, employ the well-known rotating wave approximation (see the supplementary material). The calculations with the full Hamiltonian in Eq. (1) support these two steps. The resulting simplified Hamiltonian takes on the form

$$\hat{H}^D(t) = \left(-\frac{1}{2M_r}\frac{\partial^2}{\partial R^2} + \frac{1}{2M_r R^2}L_\theta^2\right)\mathbf{1} + \begin{pmatrix} V_{\Sigma_1} + \hbar\omega & 0 \\ 0 & V_{\Pi_1} \end{pmatrix} - E_0 \cdot \sin^2(\pi t/T)\begin{pmatrix} 0 & \frac{\mu_{\Sigma_1\Pi_1}\sin\theta}{2} \\ \frac{\mu_{\Sigma_1\Pi_1}\sin\theta}{2} & 0 \end{pmatrix}. \quad (2)$$

In this picture, the laser light shifts the energy of the Σ_1 ground potential curve by $\hbar\omega$ and a crossing between the shifted ground ($V_{\Sigma_1}+\hbar\omega$) and the excited (V_{Π_1}) potential energy curves is created [Fig. 1(a)].

By diagonalizing the potential energy matrix [second + third terms in Eq. (2)], one obtains the adiabatic lower and upper potential surfaces[27] seen in Fig. 1(c) for the maximum of the pulse. These two surfaces cross giving rise to conical intersections whenever the conditions $\sin\theta = 0 (\theta = 0, \theta = \pi)$ and $V_{\Sigma_1} + \hbar\omega = V_{\Pi_1}$ are simultaneously fulfilled. For the parallel transition, the $\sin\theta$ factors are replaced by $\cos\theta$ in Eqs. (1) and (2). Consequently, the internuclear LICI position R is unaffected, but the angular criterion is modified to $\cos\theta = 0 (\theta = \pi/2)$. Namely, for perpendicular transitions, the LICIs occur at $\theta = 0; \theta = \pi$, while for parallel transitions, at $\theta = \pi/2$.

The dressed adiabatic surfaces of the model are similar to those in other parallel transition cases[18,26] and are shown in the supplementary material. We stress again that it is Eq. (1) which is used in the dynamical simulations, and Eq. (2) is used to provide the pictorial tool for the understanding of the LICI phenomenon. We add, however, that the dynamical results obtained with Eq. (1) are very similar to those obtained with Eq. (2).

The MCTDH (multi configurational time-dependent Hartree) method[39–43] has been used to solve the time-dependent Schrödinger-equation. The R degree of freedom (DOF) was defined on a sin-DVR (discrete variable representation) grid (N_R basis elements for $R = 1.058$–21.16 Å). The rotational DOF, θ, was described by N_θ Legendre-polynomials, $P_l^m(\cos\theta)$, with $m = 0$ and $l = 0, 1, \ldots, N_\theta - 1$. In the MCTDH wave function representation, these primitive basis sets (χ) are then used to construct the single particle functions (ϕ) whose time-dependent linear combinations form the total nuclear wavepacket (ψ),

$$\phi_{j_q}^{(q)}(q,t) = \sum_{i=1}^{N_q} c_{j_q i}^{(q)}(t)\chi_i^{(q)}(q), \quad q = R,\ \theta,$$
$$\psi(R,\theta,t) = \sum_{j_R=1}^{n_R}\sum_{j_\theta=1}^{n_\theta} A_{j_R j_\theta}(t)\phi_{j_R}^{(R)}(R,t)\phi_{j_\theta}^{(\theta)}(\theta,t). \quad (3)$$

The actual number of basis functions were $N_R = 1024$ and $N_\theta = 61, 301, 501$ for the vibrational and rotational DOFs, respectively. The number of single particle functions for both DOF on the Σ_1 and Π_1 electronic states was ranging from 10 to 18 and 10 to 24, respectively. The values of N_θ and $n_R = n_\theta$ were chosen depending on the peak laser intensity so as to provide proper convergence. In order to minimize unwanted reflections and transmissions caused by the finite length of the R-grid, complex absorbing potentials (CAP) have been employed at the end of the grid (last 5.29 Å). The dissociating nuclear wavepacket absorbed by the CAP has been applied to calculate the angular distribution of the photofragments,

$$P(\theta_j) = \frac{1}{w_j}\int_0^\infty \langle\psi(R,\theta,t)|W_{\theta_j}|\psi(R,\theta,t\rangle dt. \quad (4)$$

In Eq. (4), w_j is the weight factor corresponding to the relevant grid point in the applied DVR and $-iW_{\theta_j}$ is the projection of the CAP on a specific grid point associated with the rotational DOF. To calculate the potential energy and dipole moment curves presented in Fig. 1, the Molpro[44] package has been utilized. These quantities were calculated at the MRCI/aug-cc-pVQZ level of theory based on four-state-averaged CASSCF/aug-cc-pVQZ computations and good agreement with other studies[31] has been achieved.

In our simulations, the following scenario is considered. The system, initially in the lowest rovibrational eigenstate of Σ_1, is excited to Π_1 with a single resonant laser pulse duration of $T = 80$ fs and a carrier frequency 6.56 eV [see Fig. 1(a)]. As a result, the molecule directly dissociates into Mg^+ and H fragments for which the angular distributions are shown in Fig. 2. Here, the results for 1D and 2D simulations are compared for both the model [Figs. 2(a) and 2(c)] and the real

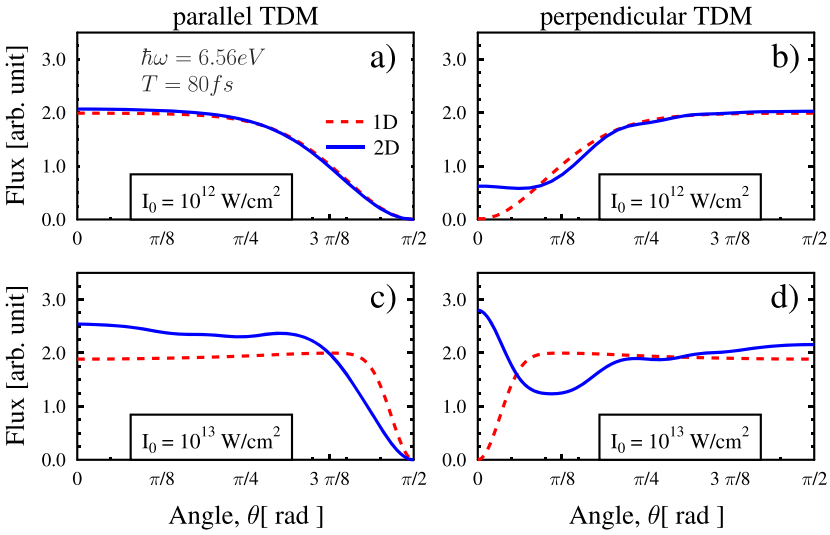

FIG. 2. Angular distributions of the MgH^+ photofragments dissociating on Π_1, computed in 1D (red dashed lines) and 2D (blue solid lines). Results for the parallel (left panels) and perpendicular transitions (right panels) are compared for two intensities.

system [Figs. 2(b) and 2(d)]. Let us first discuss the model system. As seen in Fig. 2(a), at low intensity, no dissociation occurs at $\theta = \pi/2$ and a qualitatively similar behavior is revealed in both 1D and 2D. However, upon increasing the intensity, the molecules are rotated toward the parallel direction in 2D, leading to a generally more bumpy structure compared to the 1D case where the molecules do not rotate [Fig. 2(c)]. Similar observations were found recently in the photodissociation of the D_2^+ and H_2^+ molecular ions.[17,24]

In sharp contrast to the model system, remarkable *qualitative* differences between 1D and 2D are clearly seen in the real system. The angular distributions obtained in the 1D description exhibit perfect mirror images of those computed for the model system reflecting the different TDM orientations in the two calculations. However, in the 2D description, where the molecules can be dynamically rotated by the field, a completely unexpected trend is revealed. Here, a non-negligible amount of dissociation occurs in the vicinity of $\theta = 0$ even at low intensity, which is further enhanced at stronger couplings. In spite of the zero dipole coupling at $\theta = 0$, the MgH^+ ions tend to dissociate in this direction in the Π_1 electronic state. This finding is in total contrast to the 1D results where no dissociation at all is predicted for $\theta = 0$!

The robust dissociation occurring at $\theta = 0$ in 2D [Figs. 2(b) and 2(d)] cannot be explained without the strong nonadiabatic effects due to the existence of the LICI. In MgH^+, the LICI occurs at $\theta = 0$ (and $\theta = \pi$), while for the model at $\theta = \pi/2$. According to the energetic landscape of the light-dressed upper adiabatic potential energy surfaces [see Fig. 1(c)], the excited system is rotated towards the $\theta = 0$ and $\theta = \pi$ directions. At $\theta = 0$ and $\theta = \pi$, the LICI becomes responsible for the significant dissociation in these directions (note the zero coupling at this angle). In other words, the strong nonadiabaticity introduced by the intense field turns the molecules parallel to the polarization direction which can then travel through the LICI to the lower adiabatic surface on which they dissociate.

This behavior is illustrated in Fig. 3, where the total nuclear density ($|\psi(R,\theta,t)|^2 = |\psi_{\Sigma_1}(R,\theta,t)|^2 + |\psi_{\Pi_1}(R,\theta,t)|^2$) is presented for several time moments (for the individual diabatic state nuclear densities and populations, see the supplementary material). Here, the laser pulse is centered around $t = 40$ fs, and the higher intensity is applied in order to better visualize the induced strong nonadiabatic effects ($I_0 = 10^{13}$ W/cm^2). According to the intensity profile of the laser pulse, the laser-induced nonadiabaticity and the dressed adiabatic potentials vary in time. After some initial propagation of the density in the direction about $\theta = \pi/2$ [Figs. 3(a) and 3(b)] which is attributed to the isotropic initial distribution ($J = 0$), new peaks start to develop at $\theta = 0$ and $\theta = \pi$ directions [Fig. 3(c)]. These peaks intensify at later times and become responsible for the pronounced peaks found in the angular distribution in Fig. 2(d). The appearance of the peaks in the close vicinity of the LICIs (denoted by white crosses in Fig. 3) coincides with the temporal maxima of the laser pulse, namely, when the nonadiabatic effects are the strongest. This confirms that the significant peaks found in the angular distributions originate from population transfers that take place via the LICIs.

The essence of these findings can also be interpreted with the help of selection rules. Accordingly, odd J value wavepacket components are excited to Π_1 in the "parallel TDM" situation ($\langle Y_0|\cos\theta|Y_J\rangle$), while for the "perpendicular TDM" case, even J values appear ($\langle Y_0|\sin\theta|Y_J\rangle$). As the odd Legendre-polynomials of $\cos\theta$ all have a node at $\cos\theta = 0$, i.e., $\theta = \pi/2$, the local density on Π_1 vanishes there, while no such kind of behavior happens for even J components. Consequently, no dissociation is expected at $\theta = \pi/2$ for the "parallel TDM" situation, and the dissociation can occur at any angle for the "perpendicular TDM" case as seen in Fig. 2. We mention that due to the strong nonadiabatic effects, J values up to about 14 are found to be populated after the pulse has expired.

A few words about the role of permanent dipoles: We note that they cannot affect the angular LICI position, but can perturb the internuclear R position of the LICI in the case of perpendicular transitions. In the present investigation, the impact of these moments has been found to be

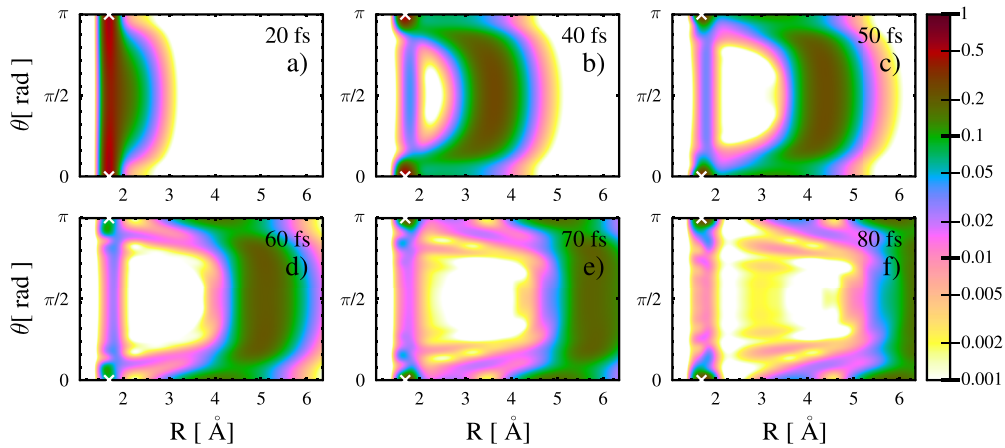

FIG. 3. Time-evolution of the MgH^+ nuclear density induced by a $T = 80$ fs long laser pulse of $\hbar\omega = 6.56$ eV energy and $I_0 = 10^{13}$ W/cm^2 peak intensity. The sin-square shape pulse is centered around 40 fs, hence the snapshots follow the $\Sigma_1 \rightarrow \Pi_1$ population transfer mediated by the LICIs at $\theta = 0$ and $\theta = \pi$ (denoted by white crosses). All the panels show the results of 2D calculations.

negligible, but in strongly polar molecules, they can have an impact on the laser-induced nonadiabatic dynamics. As they are parallel to the molecular axis, the field tends to rotate strongly polar molecules to become parallel to the laser polarization. In the case of parallel transitions, this will further suppress nonadiabatic effects as the wavepacket moves away from the LICI, but in the case of perpendicular transitions, the field will further push the wavepacket in the direction of the LICI and a significant enhancement of the nonadiabatic effects is expected.

In summary, the obtained results undoubtedly demonstrate the direct impact of the laser-induced conical intersections on the dissociation dynamics of MgH^+. The structure of the angular distributions at $\theta = 0$ reveals strong nonadiabatic effects caused by the LICI. The molecules rotated by the field parallel to the polarization direction can travel through the LICI and dissociate on the lower adiabatic surface. We hope that the reported significant impact of the TDM orientation on the dynamics and the resulting angular distribution of the dissociating photofragments will find experimental realizations.

See supplementary material for (i) the rotating wave approximation transformation steps, (ii) the dressed adiabatic potential energy surfaces of the model system, and (iii) the individual diabatic state nuclear densities and populations.

The authors thank Markus Kowalewski for the fruitful discussions. This research was supported by the EU-funded Hungarian Grant No. EFOP-3.6.2-16-2017-00005. The authors are grateful to NKFIH for support (Grant No. K128396). We acknowledge financial support by the Deutsche Forschungsgemeinschaft (Project ID No. CE10/50-3). This material is based upon work supported in part by the U.S. ARL and the U.S. ARO under Grant No. W911NF-14-1-0383.

[1]E. Teller, J. Phys. Chem. **41**, 109 (1937).
[2]H. Köppel, W. Domcke, and L. S. Cederbaum, Adv. Chem. Phys. **57**, 59 (1984).
[3]W. Domcke, D. Yarkony, and H. Köppel, *Conical Intersections* (World Scientific, New Jersey, 2004).
[4]G. A. Worth and L. S. Cederbaum, Annu. Rev. Phys. Chem. **55**, 127 (2004).
[5]M. Baer, *Beyond Born-Oppenheimer: Electronic Non-Adiabatic Coupling Terms and Conical Intersections* (Wiley, New York, 2006).
[6]H. Nakamura, *Nonadiabatic Transition: Concepts, Basic Theories and Applications*, 2nd ed. (World Scientific, Singapore, 2012).
[7]K. Takatsuka, T. Yonehara, K. Hanasaki, and Y. Arasaki, *Chemical Theory beyond the Born-Oppenheimer Paradigm: Nonadiabatic Electronic and Nuclear Dynamics in Chemical Reactions* (World Scientific Publishing, New Jersey, 2015).
[8]E. E. Aubanel and A. D. Bandrauk, J. Phys. Chem. **97**, 12620 (1993).
[9]B. J. Sussman, D. Townsend, M. Yu, and A. S. Ivanov, Science **314**, 278 (2006).
[10]N. Moiseyev, M. Sindelka, and L. S. Cederbaum, J. Phys. B: At., Mol. Opt. Phys. **41**, 221001 (2008).
[11]M. Sindelka, N. Moiseyev, and L. S. Cederbaum, J. Phys. B: At., Mol. Opt. Phys. **44**, 045603 (2011).
[12]G. J. Halász, Á. Vibók, M. Sindelka, N. Moiseyev, and L. S. Cederbaum, J. Phys. B: At., Mol. Opt. Phys. **44**, 175102 (2011).
[13]G. J. Halász, M. Sindelka, N. Moiseyev, L. S. Cederbaum, and Á. Vibók, J. Phys. Chem. A **116**, 2636 (2012).
[14]G. J. Halász, Á. Vibók, N. Moiseyev, and L. S. Cederbaum, J. Phys. B: At., Mol. Opt. Phys. **45**, 135101 (2012).
[15]G. J. Halász, Á. Vibók, N. Moiseyev, and L. S. Cederbaum, Phys. Rev. A **88**, 043413 (2013).
[16]G. J. Halász, A. Csehi, Á. Vibók, and L. S. Cederbaum, J. Phys. Chem. A **118**, 11908 (2014).
[17]G. J. Halász, Á. Vibók, H. D. Meyer, and L. S. Cederbaum, J. Phys. Chem. A **117**, 8528 (2013).
[18]G. J. Halász, Á. Vibók, and L. S. Cederbaum, J. Phys. Chem. Lett. **6**, 348 (2015).
[19]M. Pawlak and N. Moiseyev, Phys. Rev. A **92**, 023403 (2015).
[20]A. Csehi, G. J. Halász, L. S. Cederbaum, and Á. Vibók, Faraday Discuss. **194**, 479 (2016).
[21]L. S. Cederbaum, Y. C. Chiang, P. V. Demekhin, and N. Moiseyev, Phys. Rev. Lett. **106**, 123001 (2011).
[22]C. C. Shu, K. J. Yuan, D. Dong, I. R. Petersen, and A. D. Bandrauk, J. Phys. Chem. Lett. **8**, 1 (2017).
[23]T. Szidarovszky, G. J. Halász, A. G. Császár, L. S. Cederbaum, and Á. Vibók, J. Phys. Chem. Lett. **9**, 2739 (2018).
[24]A. Natan, M. R. Ware, V. S. Prabhudesai, U. Lev, B. D. Bruner, O. Heber, and P. H. Bucksbaum, Phys. Rev. Lett. **116**, 143004 (2016).
[25]P. V. Demekhin and L. S. Cederbaum, J. Chem. Phys. **139**, 154314 (2013).
[26]A. Csehi, G. J. Halász, L. S. Cederbaum, and Á. Vibók, J. Phys. Chem. Lett. **8**, 1624 (2017).
[27]A. Csehi, G. J. Halász, L. S. Cederbaum, and Á. Vibók, Phys. Chem. Chem. Phys. **19**, 19656 (2017).
[28]A. Tóth, P. Badankó, G. J. Halász, Á. Vibók, and A. Csehi, "Importance of the lowest-lying Π electronic state in the photodissociation dynamics of LiF," Chem. Phys. (in press).
[29]A. Bertelsen, I. S. Vogelius, S. Jørgensen, R. Kosloff, and M. Drewsen, Eur. Phys. J. D **31**, 403 (2004).
[30]S. Jørgensen, M. Drewsen, and R. Kosloff, J. Chem. Phys. **123**, 094302 (2005).
[31]S. Kahra, G. Leschhorn, M. Kowalewski *et al.*, Nat. Phys. **8**, 238 (2012).
[32]D. Leibfried, New J. Phys. **14**, 023029 (2012).
[33]P. F. Staanum, K. Højbjerre, P. S. Skyt, A. K. Hansen, and M. Drewsen, Nat. Phys. **6**, 271 (2010).
[34]J. M. Berglund, M. Drewsen, and C. P. Koch, New J. Phys. **17**, 025007 (2015).
[35]N. Deb, B. R. Heazlewood, M. T. Bell, and T. P. Softley, Phys. Chem. Chem. Phys. **15**, 14270 (2013).
[36]M. Tacconi, F. A. Gianturco, E. Yurtsever, and D. Caruso, Phys. Rev. A **84**, 013412 (2011).
[37]F. Wolf, Y. Wan, J. C. Heip, F. Gebert, C. Shi, and P. O. Schmidt, Nature **530**, 457 (2016).
[38]S. I. Chu, J. Chem. Phys. **75**, 2215 (1981).
[39]H. D. Meyer, U. Manthe, and L. S. Cederbaum, Chem. Phys. Lett. **165**, 73 (1990).
[40]M. H. Beck, A. Jäckle, G. A. Worth, and H. D. Meyer, Phys. Rep. **324**, 1 (2000).
[41]H. D. Meyer, F. Gatti, and G. A. Worth, *Multidimensional Quantum Dynamics: MCTDH Theory and Applications* (Wiley-VCH, Weinheim, 2009).
[42]*Molecular Quantum Dynamics: From Theory to Applications*, edited by F. Gatti (Springer, Berlin, Heidelberg, 2014).
[43]F. Gatti, B. Lasorne, H. D. Meyer, and A. Nauts, *Applications of Quantum Dynamics in Chemistry* (Springer, Cham, 2017).
[44]H.-J. Werner *et al.*, MOLPRO, version 2015.1, a package of *ab initio* programs, 2015, see http://www.molpro.net.